Alpha Band Dysconnectivity Networks in Major Depression during Resting State

Wenya Liu[⋆,†], Xiulin Wang[⋆,‡], Fengyu Cong[⋆,†], Timo Hämäläinen[†]
[⋆] *School of Biomedical Engineering, Faculty of Electronic Information and Electrical Engineering, Dalian University of Technology, Dalian, China*
[†] *Faculty of Information Technology, University of Jyväskylä, Jyväskylä, Finland*
[‡] *Department of Radiology, Affiliated Zhongshan Hospital of Dalian University, Dalian, China*
wenyaliu0912@foxmail.com, xiulin.wang@foxmail.com, cong@dlut.edu.cn, timo.t.hamalainen@jyu.fi

***Abstract*—Major depression disorder (MDD) is associated with abnormal variability of functional connectivity during resting state. Impaired modulations of resting alpha oscillations have been demonstrated to be an important biomarker of MDD. In this study, we investigated the alpha-band dynamic functional networks in MDD using resting state electroencephalography. To explore the dysconnectivity networks at the group level, we assume that the MDD group and the healthy group share some common temporal networks but also retain individual temporal networks. Considering the multiway structure of the data, we applied a coupled tensor decomposition model on two adjacency tensors with the dimension of time $\times$ connectivity $\times$ subject. The double-coupled constraints are imposed on temporal and adjacency modes. We summarized two alpha-band dysconnectivity networks by clustering the individual networks characterized with MDD.**

***Index Terms*—major depression, oscillatory networks, coupled tensor decomposition, dynamic connectivity**

I. Introduction

Major depression disorder (MDD) is one of the most common psychiatric disorders which impairs the affective and cognitive functions of patients [1], [2]. Many researches have demonstrated that MDD is associated with large-scale dysconnectivity of functional networks during resting state, like the default mode network (DMN) [3], [4]. The process that functional networks coalesce and dissolve overtime to support continuous cognitive tasks is termed as dynamic functional connectivity (dFC). Recently, researches have reported that MDD shows increased and decreased dFC of specific networks and cross-talk networks. [5]–[7]. Oscillations can regulate changes of functional networks [8], [9]. Impaired coordination of networks with resting alpha oscillations is notable in psychiatric disorders, like MDD [9]–[11]. In this study, we investigated the alpha band dFC in MDD using resting state electroencephalography (EEG).

In the analysis of temporal dynamics of functional connectivity for two groups with multiple subjects, the data is naturally characterized with a multidimensional structure. In addition, under the same condition, the MDD group and the healthy group share coupling information but also retain individual features for group differences [12], [13]. Matrix decomposition methods, like principal component analysis (PCA) and independent component analysis (ICA), are widely used in dFC analysis to obtain the connectivity components and the corresponding temporal profile [14]–[16]. However, matrix decomposition methods will impose uncorrelated or independent constraints and ignore the hidden interactions across different modes of multiway data. Recently, tensor decomposition methods have been applied in dFC analysis, and the applications are based on the assumption of spatial consistency, which means that the functional networks are consistent among subjects or groups [17], [18]. In this study, we introduced the coupled Canonical Polyadic decomposition (coupled CPD) model, which is a very flexible model to add desired constraints. This model can reveal the interactions between different modes and realize simultaneous extraction of common features shared among two groups and individual features specified in MDD [13], [19]. To the best of our knowledge, this is the first attempt to apply the coupled CPD model and investigate the dysconnectivity networks in MDD or other psychiatric disorders during resting state.

In our study, we proposed a low-rank double-coupled nonnegative Canonical Polyadic decomposition (DC-NCPD) model based on coupled CPD to explore the temporal dynamics of functional networks in MDD during resting state. Firstly, we extracted alpha oscillations and applied phase lag index (PLI) to construct functional connectivity networks with a sliding window technique. Then, we constructed two third-order tensors with the dimension of time $\times$ connectivity $\times$ subject for the MDD group and the healthy group. We applied the low-rank DC-NCPD model, and imposed the nonnegative constraint on each mode and the coupled constraint on temporal and adjacency modes. Finally, we clustered two dysconnectivity networks from individual features in MDD.

In this paper, scalars, vectors, matrices and tensors are denoted by lowercase, boldface lowercase, boldface uppercase and boldface script letters, respectively, e.g., x, $\boldsymbol{x}$, $\boldsymbol{X}$, $\boldsymbol{\mathcal{X}}$. Indices range from 1 to their capital version, e.g., $i = 1, \cdots, I$.

This work was supported by National Natural Science Foundation of China (Grant No.91748105), National Foundation in China (No. JCKY2019110B009 & 2020-JCJQ-JJ-252), the Fundamental Research Funds for the Central Universities [DUT2019 & DUT20LAB303] in Dalian University of Technology in China, and the scholarships from China scholarship Council (No.201706060263). (Corresponding author: Fengyu Cong.)

II. METHODS

A. Data Description and Preprocessing

We used the Multi-modal Open Dataset for Mental-disorder Analysis (MODMA dataset) which was an open access dataset [20]. Twenty-four MDD subjects and twenty-nine healthy control (HC) subjects were recruited in the experiment. Five minutes eye-closed resting state EEG signals were recorded by a 128-channel HydroCel Geodesic Sensor Net (Electrical Geodesics Inc., Oregon Eugene, USA) with the sampling frequency of 250 Hz. We preprocessed the data with EEGLAB toolbox [21]. The data were filtered to alpha band (8-13 Hz) with a FIR band-pass filter and re-referenced with average reference. Eye movement artifacts were removed by ICA, bad channels were interpolated by spherical interpolations, and bad time points were removed continuously. After preprocessing, the three minutes EEG data with twenty-two MDD subjects and twenty-four HC subjects were remained for further analysis.

B. Dynamic functional connectivity

The EEG data were segmented into $T = 178$ windows by a sliding window with the window length of 3 s and the overlap of 2 s. Then, to reduce the influence of source leakage, PLI was applied to calaulate the functional connectivity [22]. Within each time window and each subject, the PLI value of channel i and channel j can be computed as:

$$PLI_{i,j} = |< sign(\varphi_i - \varphi_j >|, \tag{1}$$

where φ_i and φ_j mean the instantaneous phases calculated by Hilbert transform of channel i and channel j.

Then, we can construct two adjacency tensors with the dimension of time $\times$ connectivity $\times$ subject, $\boldsymbol{\mathcal{X}}^{\text{HC}} \in \mathbb{R}^{T\times N\times S_{\text{HC}}}$ ($178 \times 8128 \times 24$) for the HC group and $\boldsymbol{\mathcal{X}}^{\text{MDD}} \in \mathbb{R}^{T\times N\times S_{\text{MDD}}}$ ($178 \times 8128 \times 22$) for the MDD group, where $N = 128 \times (128-1)/2$ represents the number of unique connections. $S_{\text{HC}} = 24$ and $S_{\text{MDD}} = 22$ mean the number of subjects in the HC group and the MDD group, respectively.

C. Coupled Canonical Polyadic Decomposition

1) Low-rank double-coupled nonnegative Canonical Polyadic decomposition: For two third-order tensors $\boldsymbol{\mathcal{X}}^{\text{HC}} \in \mathbb{R}^{T\times N\times S_{\text{HC}}}$ and $\boldsymbol{\mathcal{X}}^{\text{MDD}} \in \mathbb{R}^{T\times N\times S_{\text{MDD}}}$, we impose coupled constraints on temporal and adjacency modes. The DC-NCPD model can be represented by minimizing the following objective function:

$$\begin{aligned}\mathcal{J}(\boldsymbol{u}_r^{(n)}, \boldsymbol{v}_r^{(n)}) = \|\boldsymbol{\mathcal{X}}^{\text{HC}} - \sum_{r=1}^{R_{\text{HC}}} \boldsymbol{u}_r^{(1)} \circ \boldsymbol{u}_r^{(2)} \circ \boldsymbol{u}_r^{(3)}\|_F^2 \\ + \|\boldsymbol{\mathcal{X}}^{\text{MDD}} - \sum_{r=1}^{R_{\text{MDD}}} \boldsymbol{v}_r^{(1)} \circ \boldsymbol{v}_r^{(2)} \circ \boldsymbol{v}_r^{(3)}\|_F^2 \\ \text{s.t. } \boldsymbol{u}_r^{(1)} = \boldsymbol{v}_r^{(1)} (r \le L_t),\ \boldsymbol{u}_r^{(2)} = \boldsymbol{v}_r^{(2)} (r \le L_c).\end{aligned} \tag{2}$$

where R_{HC} and R_{MDD} are the ranks of $\boldsymbol{\mathcal{X}}^{\text{HC}}$ and $\boldsymbol{\mathcal{X}}^{\text{MDD}}$, and $\circ$ denotes the vector outer product. $\boldsymbol{u}_r^{(n)}$ and $\boldsymbol{v}_r^{(n)}$ denote the rth component of factor matrices $\boldsymbol{U}^{(n)}$ and $\boldsymbol{V}^{(n)}$, $n = 1, 2, 3$, in the modes of time, connectivity and subject for two groups. $\|\cdot\|_F$ denotes the Frobenius norm. L_t and L_c denote the number of components coupled in temporal and adjacency modes, and $L_{t,c} \le \min(R_{\text{HC}}, R_{\text{MDD}})$.

In this study, the fast hierarchical alternative least squares (FHALS) algorithm is applied to optimize the DC-NCPD problem in (2) [13], [23]. To reduce the computational complexity, the low-rank approximation by the alternative least squares (ALS) algorithm is introduced before FHALS optimization. We suppose that the rank-$\tilde{R}_{\text{HC}}$ approximation of $\boldsymbol{\mathcal{X}}^{\text{HC}}$ and the rank-$\tilde{R}_{\text{MDD}}$ approximation of $\boldsymbol{\mathcal{X}}^{\text{MDD}}$ obtained by unconstrained ALS are expressed as $[\![\tilde{\boldsymbol{U}}^{(1)}, \tilde{\boldsymbol{U}}^{(2)}, \tilde{\boldsymbol{U}}^{(3)}]\!]$ ($\tilde{R}_{\text{HC}} \le R_{\text{HC}}$) and $[\![\tilde{\boldsymbol{V}}^{(1)}, \tilde{\boldsymbol{V}}^{(2)}, \tilde{\boldsymbol{V}}^{(3)}]\!]$ ($\tilde{R}_{\text{MDD}} \le R_{\text{MDD}}$), respectively. With the FHALS algorithm, the minimization problem in (2) can be converted into $\max(R_{\text{HC}}, R_{\text{MDD}})$ rank-1 subproblems, which can be solved sequentially and iteratively. For the rth subproblem, the learning rules of $\boldsymbol{u}_r^{(n)}$ and $\boldsymbol{v}_r^{(n)}$ can be formulated as:

$$\boldsymbol{u}_r^{(n)} = \boldsymbol{u}_r^{(n)} + \left[\tilde{\boldsymbol{U}}^{(n)}\tilde{\boldsymbol{\Gamma}}_r^{(n)} - \boldsymbol{U}^{(n)}\boldsymbol{\Gamma}_r^{(n)}\right] / \boldsymbol{\Gamma}_{(r,r)}^{(n)}, \tag{3}$$

and

$$\boldsymbol{v}_r^{(n)} = \boldsymbol{v}_r^{(n)} + \left[\tilde{\boldsymbol{V}}^{(n)}\tilde{\boldsymbol{\Lambda}}_r^{(n)} - \boldsymbol{V}^{(n)}\boldsymbol{\Lambda}_r^{(n)}\right] / \boldsymbol{\Lambda}_{(r,r)}^{(n)}, \tag{4}$$

where $\tilde{\boldsymbol{\Gamma}}^{(n)} = [\tilde{\boldsymbol{U}}^T\boldsymbol{U}]^{\circledast -n}$, $\boldsymbol{\Gamma}^{(n)} = \left[\boldsymbol{U}^T\boldsymbol{U}\right]^{\circledast -n}$, $\tilde{\boldsymbol{\Lambda}}^{(n)} = [\tilde{\boldsymbol{V}}^T\boldsymbol{V}]^{\circledast -n}$, and $\boldsymbol{\Lambda}^{(n)} = \left[\boldsymbol{V}^T\boldsymbol{V}\right]^{\circledast -n}$. $\circledast$ denote the Hadamard (element-wise) product.

Specially, if $r \le L_t$, $\boldsymbol{u}_r^{(1)} = \boldsymbol{v}_r^{(1)}$, and if $r \le L_c$, $\boldsymbol{u}_r^{(2)} = \boldsymbol{v}_r^{(2)}$, thus their solutions should be calculated as:

$$\begin{aligned}&\boldsymbol{u}_r^{(1)} = \boldsymbol{v}_r^{(1)} = \boldsymbol{u}_r^{(1)} + \\ &\left[\tilde{\boldsymbol{U}}^{(1)}\tilde{\boldsymbol{\Gamma}}_r^{(1)} - \boldsymbol{U}^{(1)}\boldsymbol{\Gamma}_r^{(1)} + \tilde{\boldsymbol{V}}^{(1)}\tilde{\boldsymbol{\Lambda}}_r^{(1)} - \boldsymbol{V}^{(1)}\boldsymbol{\Lambda}_r^{(1)}\right] / \left[\boldsymbol{\Gamma}_{(r,r)}^{(1)} + \boldsymbol{\Lambda}_{(r,r)}^{(1)}\right],\end{aligned} \tag{5}$$

and

$$\begin{aligned}&\boldsymbol{u}_r^{(2)} = \boldsymbol{v}_r^{(2)} = \boldsymbol{u}_r^{(2)} + \\ &\left[\tilde{\boldsymbol{U}}^{(2)}\tilde{\boldsymbol{\Gamma}}_r^{(2)} - \boldsymbol{U}^{(2)}\boldsymbol{\Gamma}_r^{(2)} + \tilde{\boldsymbol{V}}^{(2)}\tilde{\boldsymbol{\Lambda}}_r^{(2)} - \boldsymbol{V}^{(2)}\boldsymbol{\Lambda}_r^{(2)}\right] / \left[\boldsymbol{\Gamma}_{(r,r)}^{(2)} + \boldsymbol{\Lambda}_{(r,r)}^{(2)}\right],\end{aligned} \tag{6}$$

A simple "half-rectifying" nonlinear projection is applied to obtain the nonnegative components. The $\max(R_{\text{HC}}, R_{\text{MDD}})$ subproblems of $\boldsymbol{u}_r^{(n)}$ and $\boldsymbol{v}_r^{(n)}$ are optimized alternatively one after another until convergence. The FHALS-based DC-NCPD algorithm is summarized in **Algorithm** 1.

2) Selection of components: In the algorithm described above, six parameters should be selected, including the number of extracted components for ALS low-rank approximation $\tilde{R}_{\text{HC}}$ and $\tilde{R}_{\text{MDD}}$, the number of totally extracted components R_{HC} and R_{MDD}, and the number of coupled components L_t and L_c. In this study, we set $\tilde{R}_{\text{HC}} = R_{HC}$ and $\tilde{R}_{\text{MDD}} = R_{MDD}$, which are selected by performing PCA on the matricization data unfolded along the third mode for each tensor and keeping the number of components with 90% explained variance. For the selection of the coupled components number L_t and L_c, we

Algorithm 1: DC-NCPD-FHALS algorithm

Input: $\boldsymbol{\mathcal{X}}^{\text{HC}}$, $\boldsymbol{\mathcal{X}}^{\text{MDD}}$, L_t, L_c, R_{HC}, R_{MDD}, $\tilde{R}_{\text{HC}}$, $\tilde{R}_{\text{MDD}}$

Initialization: $\boldsymbol{U}^{(n)}$, $\boldsymbol{V}^{(n)}$, $n = 1, 2, 3$

Calculate $\tilde{\boldsymbol{U}}^{(n)}$, $\tilde{\boldsymbol{V}}^{(n)}$, $n = 1, 2, 3$ via unconstrained ALS

while *unconvergence* **do**

  for $n = 1, 2, 3$ **do**

    for $r = 1, 2, \cdots max(R_{HC}, R_{MDD})$ **do**

      Update $\boldsymbol{u}_r^{(n)}$, $\boldsymbol{u}_r^{(n)}$ via (3), (4), (5) and (6)

    end

  end

end

Output: $\boldsymbol{U}^{(n)}$, $\boldsymbol{V}^{(n)}$, $n = 1, 2, 3$

performed the third-order CP tensor decomposition based on the FHALS algorithm on two tensors separately, and calculated the correlation maps of extracted components between two tensors in temporal and adjacency modes, respectively. The number of highly correlated (coupled) components is selected according to the correlation maps.

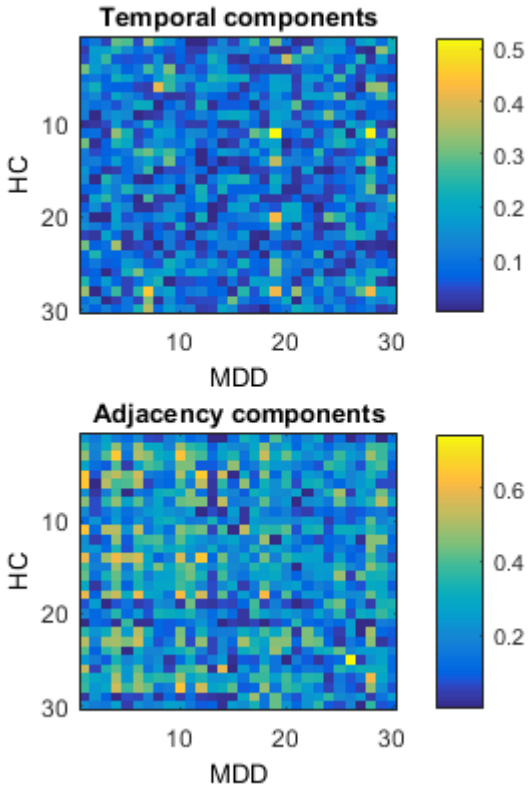

Fig. 1: The correlation maps of temporal components and adjacency components between the MDD group and the HC group.

III. Results

After PCA analysis, we set $R_{HC} = 18$ and $R_{MDD} = 17$. According to the correlation maps of temporal components and adjacency components in Fig. 1, we set $L_t = 3$ as the number of coupled components in the temporal mode and $L_c = 9$ as the number of coupled components in the adjacency mode. We applied the low-rank DC-NCPD-FHALS algorithm 30 times, and used k-means clustering to analyze the individual networks in MDD from the 30-time runs. We summarized two alpha-band dysconnectivity networks, as shown in Fig. 2. Fig. 2(I) showed a fronto-parietal network which was related to attention and emotion regulation, and Fig. 2(II) showed a frontal-occipital dysconnectivity network which also has been demonstrated to be associate with attention.

IV. Discussion and conclusion

In this study, we proposed a coupled CPD model for dFC analysis in MDD using resting EEG. We investigated the alpha-band dysconnectivity networks in MDD during resting state. For the time-varying functional connectivity calculated by the PLI method, we constructed two third-order tensors with the dimension of time $\times$ connectivity $\times$ subject. Under the assumption that common temporal functional networks were shared between the MDD group and the HC group, and individual temporal functional networks were also retained in each group, we formulated a double-coupled CPD model which was realized by the proposed low-rank DC-NCPD-FHALS algorithm. From the specific features of MDD, we summarized two overactive dysconnectivity networks in the alpha band.

We identified a fronto-parietal network, as shown in Fig. 2(I). The dysconnectivity of the fronto-parietal network has been reported in many psychiatric disorders with the impairment in cognitive control. The fronto-parietal network is associated with the top-down modulation of attention and emotion [4], [24], [25]. Many previous researches reported the overactive fronto-parietal network in MDD, which could well support our findings. Fig. 2(II) showed a frontal-occipital network which was overactive in MDD. The fronto-occipital pathways played an important role in human attention [26]. With hierarchical brain architectures, long-distance connections can mediate global integration for higher cognition [2], [27]. The dysconnectivity of the frontal-occipital network in MDD might represent the deficit in global integration for attention regulation.

The proposed model in our study fully considered the multiway structure of the temporal networks from different subjects and groups, common temporal networks between two groups, and individual temporal networks specified in each group. This framework was based on the group-level analysis. Therefore, the extracted temporal networks remained the same between all the subjects within each group. Subject differences were decomposed in residuals which were not concerned in our study.

This study applied a novel coupled CPD model for dFC analysis in MDD during resting state. The results were

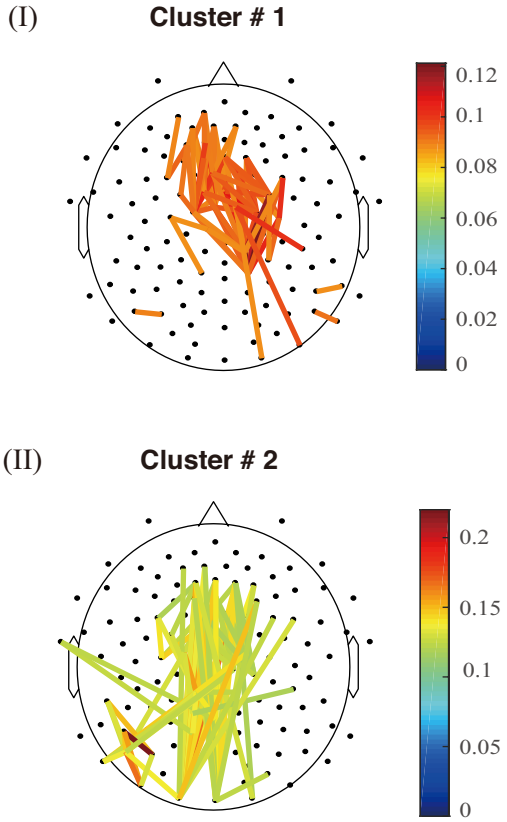

Fig. 2: The two clusters of dysconnectivity networks in MDD.

well demonstrated by previous findings, and might provide promising biomarkers in the pathoconnectomics of MDD. The proposed model can also be applied to other psychiatric disorders and different cognitive conditions.

References

[1] I. H. Gotlib and J. Joormann, "Cognition and depression: current status and future directions," *Annual review of clinical psychology*, vol. 6, pp. 285–312, 2010.

[2] W. Liu, C. Zhang, X. Wang, J. Xu, Y. Chang, T. Ristaniemi, and F. Cong, "Functional connectivity of major depression disorder using ongoing eeg during music perception," *Clinical Neurophysiology*, vol. 131, no. 10, pp. 2413–2422, 2020.

[3] Y. I. Sheline, J. L. Price, Z. Yan, and M. A. Mintun, "Resting-state functional mri in depression unmasks increased connectivity between networks via the dorsal nexus," *Proceedings of the National Academy of Sciences*, vol. 107, no. 24, pp. 11 020–11 025, 2010.

[4] R. H. Kaiser, J. R. Andrews-Hanna, T. D. Wager, and D. A. Pizzagalli, "Large-scale network dysfunction in major depressive disorder: a meta-analysis of resting-state functional connectivity," *JAMA psychiatry*, vol. 72, no. 6, pp. 603–611, 2015.

[5] M. Demirtaş, C. Tornador, C. Falcón, M. López-Solà, R. Hernández-Ribas, J. Pujol, J. M. Menchon, P. Ritter, N. Cardoner, C. Soriano-Mas *et al.*, "Dynamic functional connectivity reveals altered variability in functional connectivity among patients with major depressive disorder," *Human brain mapping*, vol. 37, no. 8, pp. 2918–2930, 2016.

[6] R. H. Kaiser, S. Whitfield-Gabrieli, D. G. Dillon, F. Goer, M. Beltzer, J. Minkel, M. Smoski, G. Dichter, and D. A. Pizzagalli, "Dynamic resting-state functional connectivity in major depression," *Neuropsychopharmacology*, vol. 41, no. 7, pp. 1822–1830, 2016.

[7] J. Wang, Y. Wang, H. Huang, Y. Jia, S. Zheng, S. Zhong, G. Chen, L. Huang, and R. Huang, "Abnormal dynamic functional network connectivity in unmedicated bipolar and major depressive disorders based on the triple-network model," *Psychological medicine*, vol. 50, no. 3, pp. 465–474, 2020.

[8] Y. Yan, T. Qian, X. Xu, H. Han, Z. Ling, W. Zhou, H. Liu, and B. Hong, "Human cortical networking by probabilistic and frequency-specific coupling," *NeuroImage*, vol. 207, p. 116363, 2020.

[9] A. A. Fingelkurts and A. A. Fingelkurts, "Altered structure of dynamic electroencephalogram oscillatory pattern in major depression," *Biological Psychiatry*, vol. 77, no. 12, pp. 1050–1060, 2015.

[10] J. A. Coan and J. J. Allen, "Frontal eeg asymmetry as a moderator and mediator of emotion," *Biological psychology*, vol. 67, no. 1-2, pp. 7–50, 2004.

[11] A. A. Fingelkurts, A. A. Fingelkurts, H. Rytsälä, K. Suominen, E. Isometsä, and S. Kähkönen, "Impaired functional connectivity at eeg alpha and theta frequency bands in major depression," *Human brain mapping*, vol. 28, no. 3, pp. 247–261, 2007.

[12] W. Liu, X. Wang, J. Xu, Y. Chang, T. Hamalainen, and F. Cong, "Identifying oscillatory hyperconnectivity and hypoconnectivity networks in major depression using coupled tensor decomposition," *bioRxiv*, 2021.

[13] X. Wang, W. Liu, P. Toiviainen, T. Ristaniemi, and F. Cong, "Group analysis of ongoing eeg data based on fast double-coupled nonnegative tensor decomposition," *Journal of neuroscience methods*, vol. 330, p. 108502, 2020.

[14] N. Leonardi, J. Richiardi, M. Gschwind, S. Simioni, J.-M. Annoni, M. Schluep, P. Vuilleumier, and D. Van De Ville, "Principal components of functional connectivity: a new approach to study dynamic brain connectivity during rest," *NeuroImage*, vol. 83, pp. 937–950, 2013.

[15] G. C. O'Neill, P. K. Tewarie, G. L. Colclough, L. E. Gascoyne, B. A. Hunt, P. G. Morris, M. W. Woolrich, and M. J. Brookes, "Measurement of dynamic task related functional networks using meg," *NeuroImage*, vol. 146, pp. 667–678, 2017.

[16] Y. Zhu, C. Zhang, H. Poikonen, P. Toiviainen, M. Huotilainen, K. Mathiak, T. Ristaniemi, and F. Cong, "Exploring frequency-dependent brain networks from ongoing eeg using spatial ica during music listening," *Brain Topography*, pp. 1–14, 2020.

[17] Y. Zhu, J. Liu, C. Ye, K. Mathiak, P. Astikainen, T. Ristaniemi, and F. Cong, "Discovering dynamic task-modulated functional networks with specific spectral modes using meg," *NeuroImage*, p. 116924, 2020.

[18] Y. Zhu, J. Liu, K. Mathiak, T. Ristaniemi, and F. Cong, "Deriving electrophysiological brain network connectivity via tensor component analysis during freely listening to music," *IEEE Transactions on Neural Systems and Rehabilitation Engineering*, 2019.

[19] G. Zhou, Q. Zhao, Y. Zhang, T. Adalı, S. Xie, and A. Cichocki, "Linked component analysis from matrices to high-order tensors: Applications to biomedical data," *Proceedings of the IEEE*, vol. 104, no. 2, pp. 310–331, 2016.

[20] H. Cai, Y. Gao, S. Sun, N. Li, F. Tian, H. Xiao, J. Li, Z. Yang, X. Li, Q. Zhao *et al.*, "Modma dataset: a multi-modal open dataset for mental-disorder analysis," *arXiv preprint arXiv:2002.09283*, 2020.

[21] A. Delorme and S. Makeig, "Eeglab: an open source toolbox for analysis of single-trial eeg dynamics including independent component analysis," *Journal of neuroscience methods*, vol. 134, no. 1, pp. 9–21, 2004.

[22] C. J. Stam, G. Nolte, and A. Daffertshofer, "Phase lag index: assessment of functional connectivity from multi channel eeg and meg with diminished bias from common sources," *Human brain mapping*, vol. 28, no. 11, pp. 1178–1193, 2007.

[23] A. Cichocki and A.-H. Phan, "Fast local algorithms for large scale nonnegative matrix and tensor factorizations," *IEICE transactions on fundamentals of electronics, communications and computer sciences*, vol. 92, no. 3, pp. 708–721, 2009.

[24] J. L. Vincent, I. Kahn, A. Z. Snyder, M. E. Raichle, and R. L. Buckner, "Evidence for a frontoparietal control system revealed by intrinsic functional connectivity," *Journal of neurophysiology*, vol. 100, no. 6, pp. 3328–3342, 2008.

[25] A. E. Whitton, S. Deccy, M. L. Ironside, P. Kumar, M. Beltzer, and D. A. Pizzagalli, "Electroencephalography source functional connectivity reveals abnormal high-frequency communication among large-scale functional networks in depression," *Biological Psychiatry: Cognitive Neuroscience and Neuroimaging*, vol. 3, no. 1, pp. 50–58, 2018.

[26] F. Doricchi, M. T. de Schotten, F. Tomaiuolo, and P. Bartolomeo, "White matter (dis) connections and gray matter (dys) functions in visual neglect: gaining insights into the brain networks of spatial awareness," *cortex*, vol. 44, no. 8, pp. 983–995, 2008.

[27] H.-J. Park and K. Friston, "Structural and functional brain networks: from connections to cognition," *Science*, vol. 342, no. 6158, 2013.